Materials Research. 2017; 20(4): 962-972
DOI: http://dx.doi.org/10.1590/1980-5373-MR-2016-0878

Evolution of TiO_2 Nanotubular Morphology Obtained in Ethylene Glycol/Glycerol Mixture and its Photoelectrochemical Performance

Alexander Bervian[a], Eliane Coser[a,b]*, Sherdil Khan[a], Sidnei Antonio Pianaro[b], Cesar Aguzzoli[c], Jossano Saldanha Marcuzzo[d], Mauricio Ribeiro Baldan[d], Célia de Fraga Malfatti[a]

[a] Laboratório de Pesquisa em Corrosão - LAPEC, Programa de Pós-Graduação em Engenharia de Minas, Metalúrgica e de Materiais - PPGE3M, Universidade Federal do Rio Grande do Sul - UFRGS, Av. Bento Gonçalves, 9500, Prédio 43427, Sala 232, 91501-970, Porto Alegre, RS, Brazil.
[b] Laboratório Interdisciplinar de Materiais Cerâmicos - LIMAC, Universidade Estadual de Ponta Grossa - UEPG, Ponta Grossa, Av. Carlos Cavalcanti, 4748, PR, Brazil.
[c] Programa de Pós-Graduação em Engenharia e Ciência dos Materiais - PGMAT, Universidade de Caxias do Sul - UCS, Rua Francisco Getúlio Vargas, 1130 - Caxias do Sul, RS, Brazil.
[d] Instituto Nacional de Pesquisas Espaciais - INPE, Av. dos Astronautas, 1.758 - Jardim da Granja, São José dos Campos, SP, Brazil.

Received: November 25, 2016; Revised: April 13, 2017; Accepted: April 21, 2017.

The evolution of TiO_2 nanotubular morphology, synthesized in a mixture of fluorinated ethylene glycol and glycerol electrolyte, was studied as a function of the anodization time. The samples were characterized by FEG-SEM, XRD, XPS, UV-Vis and EIS. The formation of single-or double-walled TiO_2 nanotube structure can be efficiently controlled by the anodization time. For anodization times less than 30 minutes, a compact oxide layer is formed, followed by double-walled nanotube formation up to 120 minutes and single-walled nanotubes up to 240 minutes. XPS analyses show that the samples obtained with short anodization time have a high carbon content and oxygenated surface species compared to the longer-time anodized sample; however, binding energy peaks for Ti 2p remained invariant. The performances of TiO_2 nanotubular photoelectrodes were evaluated in photoelectrochemical water splitting where TiO_2 nanotubes anodized for 120 minutes presented the best performance that was related to their optimal morphology and charge transportation.

Keywords: *Titanium dioxide nanotubes, TiO_2, Anodization, photoelectrochemical*

1. Introduction

Nano-architectured TiO_2 semiconductors have been extensively studied in the last few decades mainly due to their advantageous properties such as high adsorption ability, excellent photoelectrochemical activities and large specific surface area[1-3]. TiO_2-based materials are widely applied in sensors[4-9], pollutant degradation[10], hydrogen generation[11], bio-applications[12,13], and photocatalysis[14-18]. Owing to their one-dimensional nature, TiO_2 nanotubes offer a high surface area (1000 $m^2 g^{-1}$) with electron diffusion higher than that of similar systems based on nanoparticles[19]. Electrochemical anodization in fluorinated electrolytes is one of the most promising and effective methods employed to obtain highly ordered nanotube arrays of TiO_2 and many other materials with controllable morphologies[20-22]. Optimizing anodic film topography and its properties are some of the main interests for smart material application[23].

By controlling parameters such as anodization potential[24-26] anodization time[27,28], temperature[22,29], as well as the electrolyte composition[30] and its pH value[31], different nanotubular structures can be obtained. The first and second generations of electrolytes were based on aqueous electrolytes containing hydrofluoric acid and fluoride salts, respectively[32,33]. In the third generation, non-aqueous, organic solvents containing fluoride ions were used; this allowed controllable TiO_2 nanotubes to be obtained due to the high viscosity of organic electrolytes[34]. The use of viscous electrolytes allows wall smoothness by damping local spikes in the flux of reaction species by locally different pH values within the tubes. However, viscous electrolytes result in to lower current density, local acidification and amount of competing chemical dissolution[35].

The main studied organic electrolytes consist of ethylene glycol[28,34,36] and glycerol[35-37]. The latter is used due to its high viscosity that influences the diffusion of ionic species, the kinetics of nanotube formation and its morphology; therefore it does not show current fluctuations during anodization. However, the chemical dissolution of TiO_2 in glycerol is slow[35,37].

Roman et al.[36] studied the influence of the applied potential and anodization time on the nanotube diameter and length. They found that the diameter tends to increase with the water content increasing in glycerol-based electrolytes[36].

* e-mail: cosereliane@yahoo.com.br

An ethylene-glycol-based electrolyte presented a higher viscosity than that of a glycerol-based one (13.1 and 11.8 cP, respectively)[35]. High viscosity solvents decrease the mobility of ionic species; thereby, decreasing the growth rate. However, anodization in these solvents helps decreasing the current fluctuations; therefore, smoother nanotube walls are formed. In case of less viscous electrolytes, the growth rate is high, but higher chemical dissolution rate of TiO_2 causes the formation of ripples on the tube walls[35,39]. These results warrant to use ethylene-glycol/glycerol mixture (where one contributes to increase the growth rate while other to obtain smooth walled nanotubes) and to investigate their effect on the evolution of nanotubular morphology. Nischk et al.[35] showed that for the same anodization potential and time, the walls of TiO_2 nanotubes obtained in a glycerol-based electrolyte are rough; those obtained in ethylene-glycol-based electrolyte are smooth. Additionally, in glycerol-based electrolytes, the outer diameter was wider and the length of the nanotubes was shorter than that of the nanotubes obtained in the ethylene-glycol-based electrolyte.

Albu et al.[38] demonstrated the formation of double-walled TiO_2 nanotubes in ethylene glycol electrolyte at a voltage of 120 V, showing the well-defined inner and outer walls in the tubular morphology. Macak et al.[39] reviewed different anodization processes for Ti-based nano-architectured morphologies. However, the focus of these studies lay on the synthesis of nanotubes rather than their photoelectrochemical performance. Despite the fact that TiO_2 nanotubes are broadly synthesized by anodization in glycerol or ethylene glycol, few studies report TiO_2 nanotubes obtained by anodization in glycerol mixed with ethylene glycol[36]. Therefore, in order to obtain an optimized nanotubular morphology, it is interesting to study the evolution of TiO_2 nanotubes in glycerol mixed with ethylene glycol solution, and to optimize them for improved photoelectrochemical applications.

The aim of this study is to identify the nano-structures formed during the anodization procedure. The effects of anodization time on the morphology, crystal structure and surface properties of the prepared nanotubes were investigated with the final aim of applying them in photoelectrochemical water splitting.

2. Experimental

Nanotubes were grown on Ti foil grade 2 - ASTM-F67[40] (99.8 - purity: wt. %, 0.7 mm thickness, Realum), with dimensions of 1 cm × 5 cm. This foil was cleaned by ultrasonication for 15 min in degreased and deionized water (DI) in sequence, and then dried under cold air. The Ti foil was used as the working electrode and a platinum foil as the counter electrode. The distance between these electrodes was about 2 cm[27]. The anodization was performed at 60 V at a potential ramp of 1 V s^{-1}, in organic electrolyte consisting a mixture of glycerol (Synth 99.5%) and ethylene glycol (Synth - purity: 99.0%) in 2:1 (v/v) ratio, containing 0.25 wt% ammonium fluoride (Synth - purity: 98.0%) dissolved in 2 wt% of distilled water. The pH of the solution was pH 4.5-5.0 and the anodization time was varied up to (a) 5 minutes, (b) 15 minutes, (c) 30 minutes, (d) 60 minutes, (e) 120 minutes, (f) 180 minutes and (g) 240 minutes. The current transient (I-t) curves for the anodization were obtained by system acquisition (Multimeter Inimipa ET-2076A) of data recorded from the source meter connected to the software TCXX. After anodization, the samples were annealed in a muffle Furnace at 450 °C for 3 h with a heating ramp of 10 ºC/min to crystallize the TiO_2 nanotubes[34].

3. Characterization

The morphology was studied with a Field Emission Gun Scanning Electron Microscope (FEG-SEM) equipment MIRA3 by TESCAN operated at 10 and 15 kV. The crystal structure was determined by X-ray diffraction (XRD) using XRD 6000 by SHIMADZU, equipped with a graphite mono-chromator and rotating copper anode operated at 40 kV and 30 mA. The X-ray source consisted of Cu radiation (1.54184 Å) selected with a Ni filter. The measurements were performed with a step of 0.04° and a counting time of 0.60 s per step. The optical properties of the TiO_2 nanotubes were investigated by UV-Vis diffuse reflectance spectroscopy using the Carry 5000 spectrophotometer. The spectra were recorded in the wavelength range of 200-800 nm and contributions from scattering were removed using Kubelka-Munk function[41,42]. The X-ray photoelectron spectrometer (XPS) was conducted using a XPS AXIS ULTRA from Krator. The measurement carried out with Al K_α radiation (1486.6 eV). Survey spectra were determined by 160 eV pass energy and the specific element pass energy was fixed at 40 eV. The element energy position was corrected using Ag energy, as a reference, obtained from a pure Ag sample.

The photoelectrochemical measurements were performed using an Autolab potentiostat (PGSTAT 100N). The experiments were performed in a quartz cell using a three-electrode setup employing TiO_2 nanotubes as the working electrode, a Pt wire as the counter electrode and an Ag/AgCl/3.5M KCl electrode as reference electrode. The Ag/AgCl reference electrode was placed in a Lugging capillary to avoid a possible contamination of the working solution by the chloride coming from the reference compartment. The electrical contacts for all of the samples were made using copper wires in a homemade airtight Teflon reactor. Before each experiment, the reference electrode was properly washed with deionized water to avoid contamination of the electrolyte with chloride ions. The linear sweep voltammetry was performed at a scan rate of 10 mV/s in the dark and under illumination. A solar simulator (Newport) incorporated with xenon lamp (Oriel) was used as a radiation source and the radiation was filtered by an AM 1.5G filter. The intensity of the light was

calibrated by a photodiode with a known responsivity to 100 mW/cm^2 (i.e. 1 sun illumination). These electrodes were thermally treated at 450 °C which contributes to avoid organic contamination. Prior to each measurement, the photoanodes were cleaned by 3 successive cyclic voltammetry scans, applying potentials from 1 V to -1 V vs Ag/AgCl with a scan rate of 50 mV/s[43,44,45]. Prior to Electrochemical impedance spectroscopy (EIS) measurements, 3 successive CV runs were carried out. The EIS experiments were performed in the same experimental setup with equal areas shown to the electrolyte for all samples. The frequency range was 100 kHz - 100 mHz with a signal amplitude of 10 mV (peak to peak). The data was acquired under 1 Sun illumination at open circuit potential (OCP) for the respective electrodes. The waiting time to stabilize the system for OCP under 1 Sun illumination was 2 min and these values were ranged from -0.75 to 0.80 V vs Ag/AgCl. For TiO_2 the stable V_{oc} values are obtained within less than 10 sec. of illumination. Since even 10 sec illumination is enough for the open circuit potential (V_{oc}) stability; however, we followed experimental protocol of giving more time to stabilize the V_{oc} under illumination before performing the EIS experiments[43,44,45]

4. Results and Discussion

Figure 1 shows the current transient (I-t) curve obtained during the maximum time period of the anodization process. At the beginning of the anodization process, up to ~5 minutes, the anodizing current density increases abruptly to a value of ca. 1.8 mA, followed by a rapid decrease. During this anodization time, the oxidation of Ti to Ti^{4+} occurs due to the hydrolysis reaction resulting in the formation of an initial oxide barrier[46,47]. In addition, during this stage, the curve essentially follows the fluoride-free case[48], and if samples are removed from the electrolyte, a compact oxide layer will be formed[46]. After the negatively-charged cation vacancies result from dissolution in the oxide, the latter migrates to the metal/oxide barrier due to the potential gradient at the interface[49].

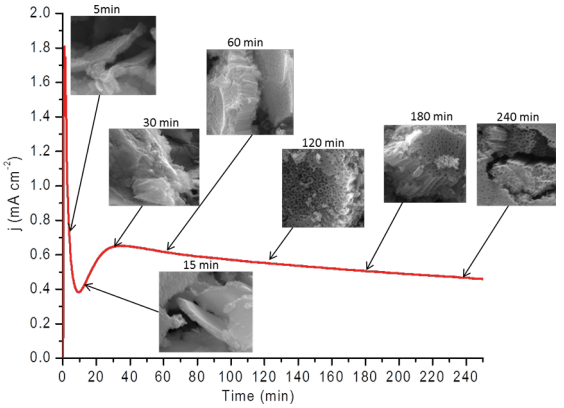

Figure 1. Current density-time behavior for titanium anodized at 60 V in 0.25 g NH_4F and 2 g H_2O for 240 minutes.

Meanwhile, the oxidation of Ti creates vacancies as well, hence facilitating the hopping of cations into the Ti vacancies[46]. This event slightly increases the current for a short time, resulting[32], in the pitting of the oxide layer due to field-assisted dissolution. In Figure 1 from 15-30 minutes, a minor increase in the current density can be clearly seen, which is related to the pitting event. Thus, irregular nanoscale pores are expected to be formed initially, which penetrate the initial compact oxide. Subsequently, a steady-state current over time can be observed after 60 minutes of anodization time. After that, the anodization current was approximately maintained at a steady value until 240 minutes (Figure 1). Compared to the literature, the current density and the time to achieve the steady state current density are slightly different to those observed in glycerol or ethylene glycol electrolytes. This is due to the fact that we have used a mixture of both of them; ethylene glycol because of its higher viscosity and higher current density, and glycerol to avoid current density fluctuations during the anodization process. We expect that the combined effect of both may be advantageous for easy growth of TiO_2 nanotubes[37]. According to Albu et al.[38] and Macak et al.[39] the synthesis of different morphologies of TiO_2 has been shown utilizing either ethylene glycol or glycerol-based electrolytes. We have used a mixture of these (viz. ethylene glycol and glycerol with a low concentration of fluoride) with the aim of investigating the evolution of tubular morphology and its applications in photoelectrochemical water splitting.

To investigate the evolution of nanotubular morphology, we conducted a series of experiments via the removal of samples after (a) 5 minutes, (b) 15 minutes, (c) 30 minutes, (d) 60 minutes, (e) 120 minutes, (f) 180 minutes and (g) 240 minutes from the anodization bath. Figure 2 shows the FEG-SEM images of the TiO_2 nanotubes prepared at different anodization times. After 5 minutes (Figure 2 (a)) of anodization, a thin oxide layer (105 nm) was formed on the surface. By increasing the anodization time to 15 and 30 minutes (Figure 2 (b) and (c), respectively), the thickness of the oxide films was increased to 218 nm and 850 nm, respectively. For the sample prepared at 30 minutes, the formation of slightly regular pits can be observed compared to those obtained at shorter time. However, tubular morphology could not be yet obtained. This may be ascribed to the fact that in these three samples, the surface barrier layer formed on the substrate surface of Ti foil is not dissolved during the anodization process, thus leading to the formation of the compact oxide layer. In addition, the I-t curve of Figure 1 clearly shows that up to ~15 minutes, the current density still decreases, and from 15 minutes to 30 minutes, a hump can be seen; yet steady current is not achieved. Thus, these conditions are not suitable for the formation of a tubular morphology.

These results are in line with the literature, as the formation of highly ordered nanotubes occurs when the current density

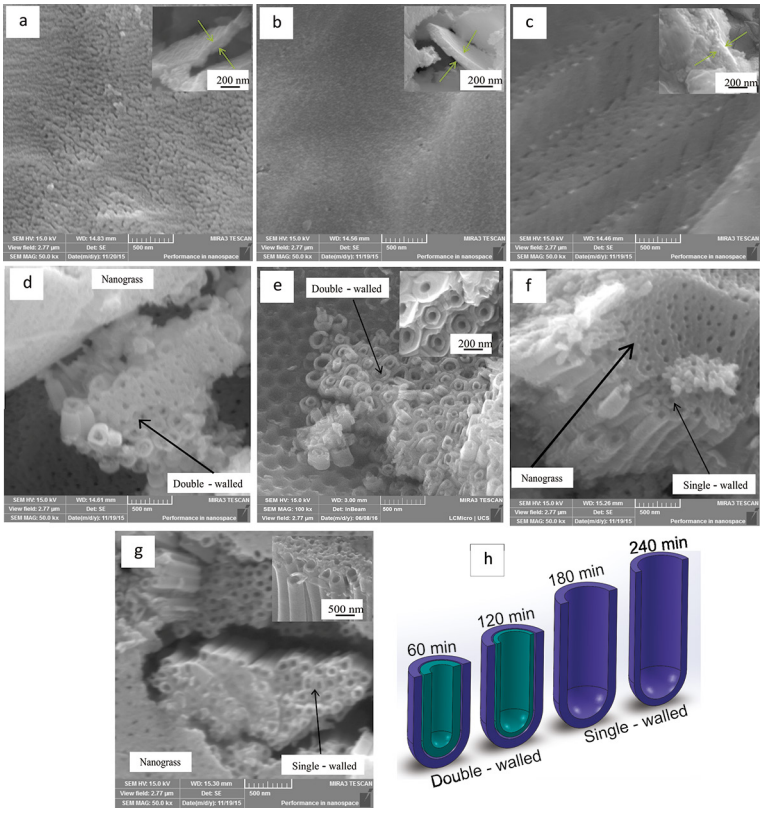

Figure 2. FEG-SEM images of TiO_2 nanotubes anodized for (a) 5 minutes, (b) 15 minutes, (c) 30 minutes, (d) 60 minutes, (e) 120 minutes, (f) 180 minutes and (g) 240 minutes. Insets show the top-view images, (h) schematic diagram showing the formation of double-walled and single-walled TiO_2 nanotubes.

becomes steady[46]. Figures 2(d)-(g) show the morphology of TiO_2 nanotubes after anodization times of 60 minutes, 120 minutes, 180 minutes and 240 minutes, respectively. In Figure 1, the current density during these anodization times remained steady, indicating that the dissolution rate is in equilibrium with the oxidation rate, and hence the formation of nanotubular morphology can be inferred[46]. These figures clearly confirm the formation of a nanotubular morphology; however, it is clear that the top layers of these samples do not show a well-defined tubular structure. It is known that during initial stage of anodization, the compact oxide, i.e., the random pore layer or the initiation layer often remains as remnants on the tube tops called nanograss and is frequently observed previously in the literature[39,50]. Efforts have been directed toward removing these layers[50-52]. Therefore, we have tried the methodology reported elsewhere to remove that layer[53,54].

Interestingly, after removal of the surface nanograss in Figures 2(d) and 2(e), a double-walled feature is revealed. The top-view images clearly show that these nanotubes are comprised of inner and outer shells. These features have been observed earlier in the literature[54]. It was found that the inner shell presented a large amount of F and C species; hence, the formation of the double-walled feature was suggested to be related to the residual amount of the trapped electrolyte species[55].

Albu et al.[38] explained the thickness of nanotubes in the form of an outer and inner shell, with a variation of thickness along the tube. Additionally, a fluoride-rich layer between the bottom of the nanotubes and the Ti substrate was observed, which was attributed to high-field migration of electrolyte anions, in particular small fluoride species that compete with O^{2-} migration[39,55,56] through the amorphous tube bottom during the tube growth. On the other hand, the double-walled features disappeared for the samples prepared at 180 and 240 minutes (Figures 2(f) and (g)) of anodization time. Therefore, single-walled or double-walled TiO_2 nanotubes can controllably be obtained by the optimizing the anodization time. In Figure 2 (e) in the bottom of the nanotubes obtained after 120 min of anodization, the formation of double-walled nanotubes can be confirmed. However, after 180 minutes of anodization (Figure (f & g)) the formation of double-wall was not observed and the outer diameter of these nanotubes is smaller than those prepared for shorter time durations; suggesting that the chemical etching occurred to dissolve the outer-wall of the nanotubes. These results indicate the effectiveness of the anodization method in producing well-defined TiO_2

nanotubes and controlling the nanotubular morphology via anodization time[57].

Figure 3 compares the cross-sectional images of the TiO_2 nanotubes obtained at 60 minutes, 120 minutes, 180 minutes, and 240 minutes of anodization times. It can be seen that the tube length increases with increasing time.

The geometrical parameters as a function of anodization time obtained from the FEG-SEM analyses are displayed in Figure 4. The length of the nanotubes increases from ~650 nm to ~6 µm, and the average length growth rate was found to be ~25 nm/min. Furthermore, the outer diameter and the inner diameter vary from 210 to 170 nm and 100 to 88 nm, respectively. This indicates that the nanotubes' diameter is extremely dependent on the anodization time[51]. The decrease in the diameters for larger anodization times can be related to the formation of single-walled nanotubes. When compared to a similar work in electrolyte without the addition of glycerol for similar anodization conditions, the nanotubes obtained here are found to be shorter; however, the outer diameter increased[26,34]. These results suggest that the addition of glycerol to the electrolyte results in decreasing the growth rate of TiO_2 nanotubes; yet it increases the diameter (Figure 4).

The as-anodized nanotubes are generally amorphous; therefore, thermal treatment is required to crystallize them[58]. Figure 5 shows the XRD patterns of the samples annealed at 450 °C for 3 h. The characteristic peak related to the anatase phase of TiO_2 appears at $2\theta = 25.2°$. The peaks at 38.3º, 40.4° and 53.4° correspond to Ti substrate KOH[30,34,58]. It should be noted that for short anodization times such as from 5-30 minutes, the characteristic anatase peak is hardly visible. On the other hand, its relative intensity compared to the Ti peaks increases with anodization time. These results are in line with the observed oxide thickness, as for long time of anodization, a thicker nanotubular layer is formed (Figure 4). The crystalline properties and optical absorption are two important factors for the photoelectrochemical performance of TiO_2 nanotubular photoanodes. Subsequently TiO_2 nanotubes with a better optical absorption and higher crystallinity will result in a better photoelectrochemical activity.

UV-Vis absorption spectra were obtained to assess the optical absorption of the TiO_2 nanotubes obtained at different anodizing times. For the sake of simplicity, UV-Vis spectra of only a few samples are shown in Figure 6. The optical bandgap energy was found to be ~3.1-3.2 eV for all samples, and is in line with the reported value for TiO_2[59,60]. It can be seen that the absorption from the sample prepared for

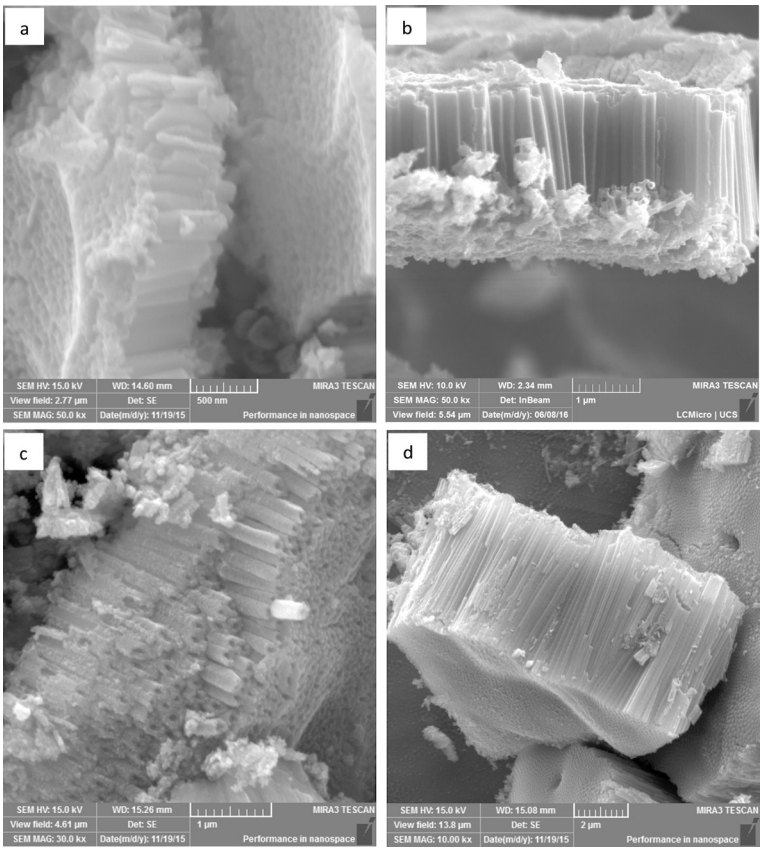

Figure 3. Cross-sectional FEG-SEM images of the TiO_2 nanotubues obtained at (a) 60 minutes, (b) 120 minutes, (c) 180 minutes and (d) 240 minutes of anodization time.

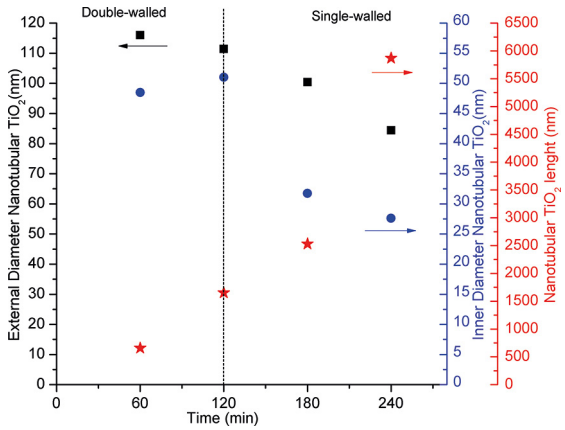

Figure 4. Diagram of nanotube inner diameter (a), external diameter (b) and length (c).

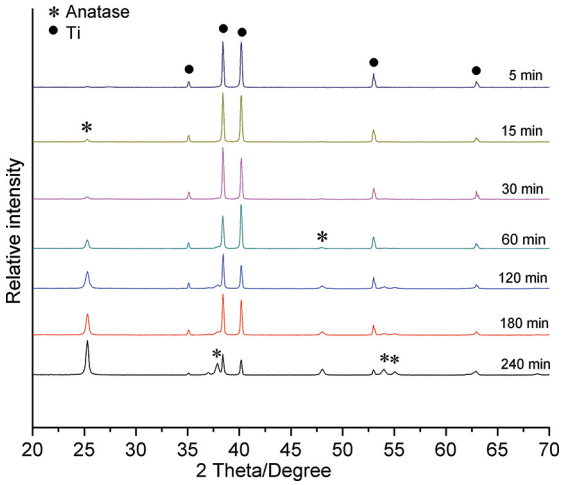

Figure 5. XRD patterns of TiO_2 samples annealed at 450 °C during 3 h with a heating and cooling rate of 10 °C min^{-1}.

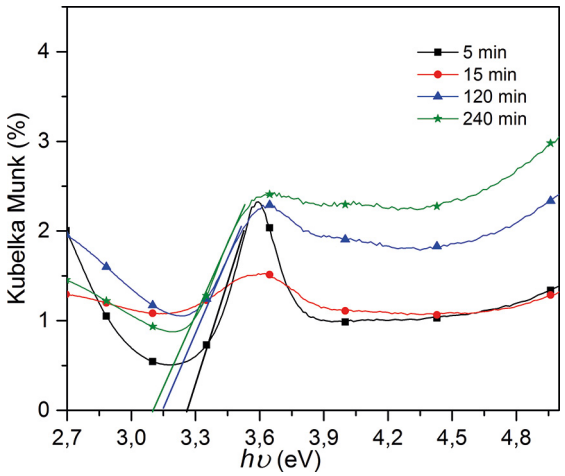

Figure 6. UV-Vis diffuse reflectance spectra of TiO_2 nanotubes obtained at different anodization times

240 minutes is higher than that prepared for shorter times of anodization. This is due to the fact that the nanotube obtained for longer times of anodization is longer (Figure 3), therefore exhibiting high absorption[59].

The XPS spectra of the TiO_2 nanotubes obtained at 5 and 120 minutes of anodization are presented in Figure 7. These spectra are obtained from the as-anodized and thermally treated samples. The survey spectra (Figure 7a) show that the dominant signals are from Ti, O and C, and the relative intensities of C1s for 5 min samples are higher than those of the samples prepared for 120 minutes. The exposure of the samples to air, as well as the anodization solution itself, can be reasons for the carbon content. However, for the anodic thin film obtained at 5 minutes, the higher carbon content might be related to the high carbon diffusion at the thin oxide/metal barrier. For the Ti 2p spectra (Figure 7b), the core lines for $2p_{1/2}$ and $2p_{3/2}$ are centered at 464 eV and oxide 455.8 eV respectively, related to Ti^{4+} [61]. For all the samples, the Ti 2p spectra do not differ in binding energies, indicating the formation of TiO_2 for the applied anodization conditions. Additionally, the deconvoluted O ls spectra (Figure 7c) present two peaks. The peak at ~531 eV corresponds to the oxide ions of the TiO_2, and another peak related to the oxygenated species at higher binding energy side centered at ~532.7 eV corresponds to the oxidized hydrocarbons. However, for the sample prepared for 5 min higher energy peak present larger area as compared to the oxide ion peak of TiO_2 (~531 eV). It may be due to the fact that for 5 min of anodization time the porous oxidized layer is thin and non-uniform; helping to incorporate higher concentration of oxygenated species from the solution to the substrate.

Subsequently, the samples obtained were tested for photoelectrochemical water splitting in 1 M KOH (aq) electrolyte under AM 1.5 G (1 sun illumination) conditions. The linear sweep voltammetry (LSV) curves are presented in Figure 8. The best photoelectrochemical performance is acquired from the sample obtained at 120 min of anodization time. Comparing its optical properties with samples prepared at longer times of anodization against their photoelectrochemical performance, it is clear that better optical absorption properties (Figure 6) and improved photoelectrochemical performance cannot be achieved simultaneously. Moreover, the photoelectrochemical performance of the sample prepared at 60 min is also better than that of samples prepared at 180 and 240 min (Figure 8). In accordance with the Beer-Lembert law, more photons will be harvested by the longer nanotubes. On the other hand, these nanotubes will have more recombination centers and higher series resistance, which result in a decreasing photoelectrochemical performance.

Thus, to ensure efficient electron collection, there should be a balance between the tube length and the optical properties of

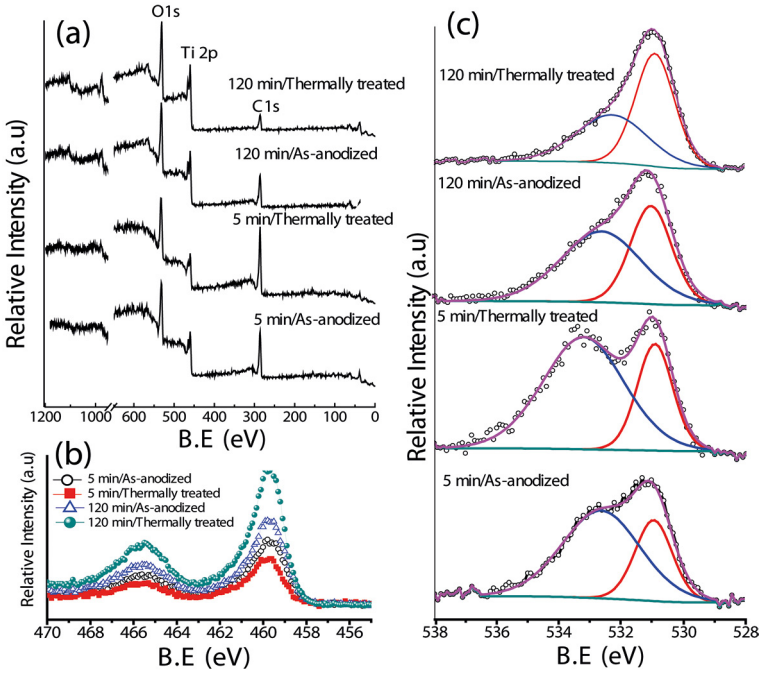

Figure 7. XPS spectra of as-anodized and thermally treated TiO_2 nanotubes; (a) survey spectra (b) Ti 2p region and (c) O 1s region.

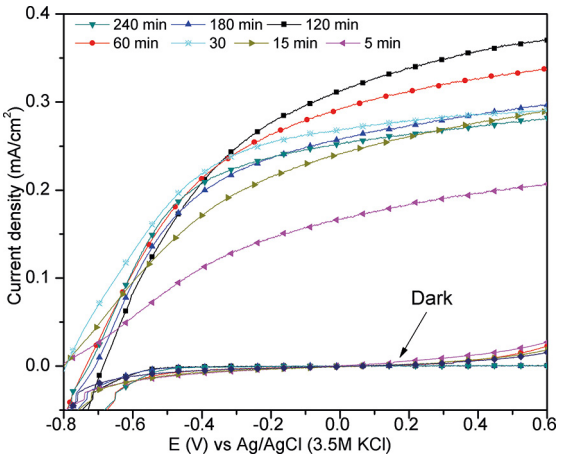

Figure 8. Linear sweep voltammetry curves of TiO_2 nanotubes obtained at different anodization times.

TiO_2 nanotubes. Furthermore, the lower photoelectrochemical performance of the samples prepared at shorter anodization times (≤ 30 min) can be rationalized on the basis of their compact morphology, resulting in a lower surface area as well as lower optical absorption abilities. Therefore, the 1D nature of TiO_2 nanotubes and their optimal light absorption are important factors in improving the photoelectrochemical performance.

To obtain further insight into the photoelectrochemical properties of TiO_2 nanotubes as a function of anodization time, the semiconductor/electrolyte interfacial charge transportation properties were investigated by electrochemical impedance spectroscopy (EIS). Figure 9 displays the Nyquist plots obtained from the TiO_2 nanotubes under AM 1.5G (1 sun illumination) conditions at open circuit potential. It can be seen that all of the samples present an incomplete semicircle, which is the characteristic of a capacitive system exhibiting non-ideal behavior. One time constant corresponding to the native passive anodic film was observed; hence, EIS data were fitted to an equivalent circuit (Figure 9) consisting of a series resistance R_s and single constant phase element (CPE) parallel with polarization resistance R_p. Based on the nanotubular morphology, i.e. porous structure, adding CPE

$$Z_{CPE} = \frac{1}{Y_0 (j\omega)^n}$$

for the TiO_2 nanotubes-electrolyte interface is physically true[20]. The impedance of the CPE is given by:

Where Y_0 is the admittance of an ideal capacitance, ω is the signal frequency and n is an empirical constant, ranging from 0-1[62-64]. Fitting the Nyquist plots into the proposed equivalent circuit, the values of the circuit elements have been deduced and are displayed in Table 1.

To visualize R_p and admittance (Y_0) of CPE as a function of anodization time better, we have plotted R_p and Y_0 against anodization time (Figure 9(b)). Y_0 increases with the anodization time (Table 1), showing that the interface becomes more capacitive; in other words, the double layer capacitance increases with anodization time. This is due

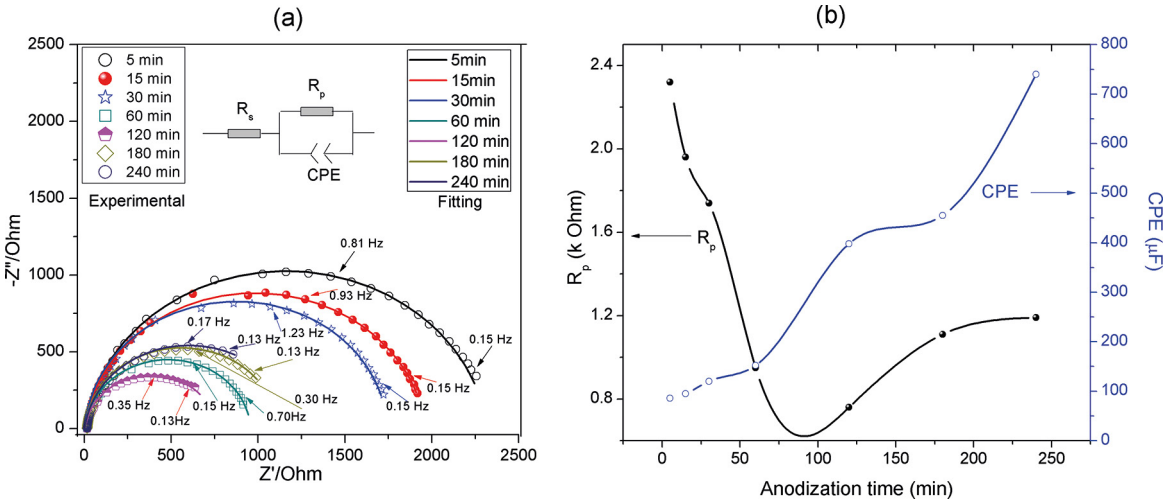

Figure 9. (a) Nyquist plots of TiO_2 nanotubes obtained at different anodization times, where the symbols represent the experimental data and the solid lines represent circuit fitting; and (b) values of R_p and Y_0 obtained from the circuit fitting as a function of anodization time.

Table 1. EIS parameters for the samples.

Anodization time	R_s(Ω)	R_p(KΩ)	Y_0/μMho	n
5 min	5.61	2.32	86	0.92
15 min	5.63	1.96	95	0.93
30 min	6.12	1.74	120	0.96
60 min	6.20	0.95	152	0.93
120 min	6.59	0.76	398	0.93
180 min	6.19	1.11	455	0.96
240 min	5.80	1.19	740	0.93

to the fact that longer nanotubes offer large area for the electrolyte; hence, capacitance increases with time.

These results corroborate the formation of a thick anodic film when the anodization time is increased; the increase in the relative intensity of the XRD peak of anatase TiO_2 (Figure 5) and an increase in the length of nanotubes from the FEG-SEM images (Figure 3) have clearly confirmed that. Furthermore, the charge transfer resistance (R_p) decreases from 5 minutes up to 120 minutes of anodization time, and then slightly increases upon any further increase in anodization time. These results are in line with the photoelectrochemical performance of these samples, as the best performance was obtained for the sample anodized for 120 minutes (Figure 8). On the other hand, the sample prepared for 5 min of anodization time had the highest charge transfer resistance as well as the lowest photocurrent response. Additionally, the samples prepared at 240 and 180 minutes had lower charge transfer resistance compared to those prepared at shorter times (≤ 30 minutes), mainly due to their large absorption as well as nanotubular nature. Hence, for improved photoelectrochemical performance, the optimal charge transportation strongly depends on the tubular morphology as well as the optical properties of the TiO_2 nanotubes. Based on the LSV curves and Nyquist plots, the sample prepared for 120 minutes of anodization time had the best photoelectrochemical properties, and has the potential to be used for technical applications.

5. Conclusions

In this work, the evolution of the tubular morphology of TiO_2 nanotubes was studied by varying anodization time in glycerol mixed ethylene glycol electrolyte-based fluorinated electrolyte. The tubular morphology was formed after 60 minutes of anodization time; before that, a compact oxide layer was observed. The diameter of the nanotubes slightly increases after 120 minutes due to the formation of single-walled nanotubes. However, their length increases linearly with anodization time. The formation of the single- or double-walled nanotubular morphology of TiO_2 is efficiently controlled by the anodization time. For improved photoelectrochemical performance from the TiO_2 nanotubes, the tube length should be sufficiently long to harvest most of the photons, yet short enough to decrease the recombination carriers. The performance of TiO_2 nanotube photoanodes evaluated in photoelectrochemical water splitting demonstrated that TiO_2 nanotubes anodized for 120 minutes presented the best performance. Also, Y_0 increased with the anodization time, showing that the interfacial capacitance increased with anodization time.

6. Acknowledgments

Thanks are due to CAPES / UDELAR (047/2013) and FAPERGS PqG (2235-2551 / 14-4) for the financial support. We also thank C-LABMU, UEPG, for carrying out the FEG-SEM analysis and LCMicro-UCS and INPE for their contribution in this work.

7. References

1. Shankar K, Bandara J, Paulose M, Wietasch H, Varghese OK, Mor GK, et al. Highly Efficient Solar Cells using TiO_2 Nanotube Arrays Sensitized with a Donor-Antenna Dye. *Nano Letters*. 2008;8(6):1654-1659.

2. Wang H, Bai Y, Zhang H, Zhang Z, Li J, Guo L. CdS Quantum Dots-Sensitized TiO_2 Nanorod Array on Transparent Conductive Glass Photoelectrodes. *The Journal of Physical Chemistry C*. 2010;114(39):16451-16455. DOI: 10.1021/jp104208z

3. Wang H, Bai Y, Wu Q, Zhou W, Zhang H, Li J, et al. Rutile TiO_2 nano-branched arrays on FTO for dye-sensitized solar cells. *Physical Chemistry Chemical Physics*. 2011;13(15):7008-7013. DOI: 10.1039/C1CP20351G

4. Du X, Wang Y, Mu Y, Gui L, Wang P, Tang Y. A New Highly Selective H_2 Sensor Based on TiO_2/PtO−Pt Dual-Layer Films. *Chemistry of Materials*. 2002;14(9):3953-3957. DOI: 10.1021/cm0201293

5. Al-Homoudi IA, Thakur JS, Naik R, Auner GW, Newaz G. Anatase TiO_2 films based CO gas sensor: Film thickness, substrate and temperature effects. *Applied Surface Science*. 2007;253(21):8607-8614. DOI: 10.1016/j.apsusc.2007.04.068

6. Li J, Zhang JZ. Optical properties and applications of hybrid semiconductor nanomaterials. *Coordination Chemistry Reviews*. 2009;253(23-24):3015-3041. DOI: 10.1016/j.ccr.2009.07.017

7. Zhao R, Xu M, Wang J, Chen G. A pH sensor based on the TiO_2 nanotube array modified Ti electrode. *Electrochimica Acta*. 2010;55(20):5647-5651. DOI: 10.1016/j.electacta.2010.04.102

8. Mun KS, Alvarez SD, Choi WY, Sailor MJ. A Stable, Label-free Optical Interferometric Biosensor Based on TiO_2 Nanotube Arrays. *ACS Nano*. 2010;4(4):2070-2076. DOI: 10.1021/nn901312f

9. Lou Z, Li F, Deng J, Wang L, Zhang T. Branch-like Hierarchical Heterostructure (α-Fe_2O_3/TiO_2): A Novel Sensing Material for Trimethylamine Gas Sensor. *ACS Applied Materials & Interfaces*. 2013;5(23):12310-12316. DOI: 10.1021/am402532v

10. Macak JM, Zlamal M, Krysa J, Schmuki P. Self-Organized TiO_2 Nanotube Layers as Highly Efficient Photocatalysts. *Small*. 2007;3(2):300-304. DOI: 10.1002/smll.200600426

11. Paulose M, Mor GK, Varghese OK, Shankar K, Grimes CA. Erratum to "Visible light photoelectrochemical and water-photoelectrolysis properties of titania nanotube arrays" [J. Photochem. Photobiol. A: Chem. 178 (2006) 8-15]. *Journal of Photochemistry and Photobiology A: Chemistry*. 2010;215(2-3):229. DOI: 10.1016/j.jphotochem.2010.08.012

12. Chen D, Zhang H, Li X, Li J. Biofunctional Titania Nanotubes for Visible-Light-Activated Photoelectrochemical Biosensing. *Analytical Chemistry*. 2010;82(6):2253-2261. DOI: 10.1021/ac9021055

13. Wang D, Liu L. Continuous Fabrication of Free-Standing TiO_2 Nanotube Array Membranes with Controllable Morphology for Depositing Interdigitated Heterojunctions. *Chemistry of Materials*. 2010;22(24):6656-6664. DOI: 10.1021/cm102622x

14. Ding Z, Lu GQ, Greenfield PF. Role of the Crystallite Phase of TiO_2 in Heterogeneous Photocatalysis for Phenol Oxidation in Water. *The Journal of Physical Chemistry B*. 2000;104(19):4815-4820. DOI: 10.1021/jp993819b

15. Kočí K, Matějů K, Obalová L, Krejčíková S, Lacný Z, Plachá D, et al. Effect of silver doping on the TiO_2 for photocatalytic reduction of CO_2. *Applied Catalysis B: Environmental*. 2010;96(3-4):239-244. DOI: 10.1016/j.apcatb.2010.02.030

16. Dongliang Y, Song Y, Zhu X, Yang R, Han A. Morphological evolution of TiO2 nanotube arrays with lotus-root-shaped nanostructure. *Applied Surface Science*. 2013;276:711-716. DOI: 10.1016/j.apsusc.2013.03.158

17. Roy SC, Varghese OK, Paulose M, Grimes CA. Toward Solar Fuels: Photocatalytic Conversion of Carbon Dioxide to Hydrocarbons. *ACS Nano*. 2010;4(3):1259-1278. DOI: 10.1021/nn9015423

18. Dong J, Han J, Liu Y, Nakajima A, Matsushita S, Wei S, et al. Defective Black TiO_2 Synthesized via Anodization for Visible-Light Photocatalysis. *ACS Applied Materials & Interfaces*. 2014;6(3):1385-1388. DOI: 10.1021/am405549p

19. Lynch RP, Ghicov A, Schmuki P. A Photo-Electrochemical Investigation of Self-Organized TiO_2 Nanotubes. *Journal of The Electrochemical Socitey*. 2010;157(3):G76-G84. DOI: 10.1149/1.3276455

20. Khan S, Teixeira SR, Santos MJL. Controlled thermal nitridation resulting in improved structural and photoelectrochemical properties from Ta_3N_5 nanotubular photoanodes. *RSC Advances*. 2015;5(125):103284-103291. DOI: 10.1039/C5RA17227F

21. Gonçalves RV, Wender H, Migowski P, Feil AF, Eberhardt D, Boita J, et al. Photochemical Hydrogen Production of Ta_2O_5 Nanotubes Decorated with NiO Nanoparticles by Modified Sputtering Deposition. *The Journal of Physical Chemistry C*. 2017;121(11):5855-5863. DOI: 10.1021/acs.jpcc.6b10540

22. Xie ZB, Blackwood DJ. Effects of anodization parameters on the formation of titania nanotubes in ethylene glycol. *Electrochimica Acta*. 2010;56(2):905-912. DOI: 10.1016/j.electacta.2010.10.004

23. Zhou X, Nguyen NT, Özkan S, Schmuki P. Anodic TiO_2 nanotube layers: Why does self-organized growth occur—A mini review. *Electrochemistry Communications.* 2014;46:157-162. DOI: 10.1016/j.elecom.2014.06.021

24. Luan X, Guan D, Wang Y. Facile Synthesis and Morphology Control of Bamboo-Type TiO_2 Nanotube Arrays for High-Efficiency Dye-Sensitized Solar Cells. *The Journal of Physical Chemistry C*. 2012;116(27):14257-14263. DOI: 10.1021/jp305280q

25. Chanmanee W, Watcharenwong A, Chenthamarakshan CR, Kajitvichyanukul P, de Tacconi NR, Rajeshwar K. Formation and Characterization of Self-Organized TiO_2 Nanotube Arrays by Pulse Anodization. *Journal of The American Chemical Society*. 2008;130(3):965-974. DOI: 10.1021/ja076092a

26. Paulose M, Shankar K, Yoriya S, Prakasam HE, Varghese OK, Mor GK, et al. Anodic Growth of Highly Ordered TiO_2 Nanotube Arrays to 134 μm in Length. *The Journal of Physical Chemistry B*. 2006;110(33):16179-16184. DOI: 10.1021/jp064020k

27. Liu Z, Zhang X, Nishimoto S, Jin M, Tryk DA, Murakami T, et al. Highly Ordered TiO_2 Nanotube Arrays with Controllable Length for Photoelectrocatalytic Degradation of Phenol. *The Journal of Physical Chemistry C*. 2008;112(1):253-259. DOI: 10.1021/jp0772732

28. Paulose M, Prakasam HE, Varghese OK, Peng L, Popat KC, Mor GK, et al. TiO_2 Nanotube Arrays of 1000 μm Length by Anodization of Titanium Foil: Phenol Red Diffusion. *The Journal of Physical Chemistry C*. 2007;111(41):14992-14997. DOI: 10.1021/jp075258r

29. Wang C, Wang M, Xie K, Wu Q, Sun L, Lin Z, et al. Room temperature one-step synthesis of microarrays of N-doped flower-like anatase TiO_2 composed of well-defined multilayer nanoflakes by Ti anodization. *Nanotechnology*. 2011;22(30):305607. DOI: 10.1088/0957-4484/22/30/305607

30. Indira K, Ningshen S, Mudali UK, Rajendran N. Effect of Anodization Temperature on the Surface Morphology of Anodized Titanium. In: Jayakumar S, Kannan MD, Balasundaraprabhu R, Prassana S, eds. *Thin Films and Nanomaterials*. Noida: Macmillan India; 2011. p. 63-66.

31. Sreekantan S, Lockman Z, Hazan R, Tasbihi M, Tong LK, Mohamed AR. Influence of electrolyte pH on TiO_2 nanotube formation by Ti anodization. *Journal of Alloys and Compounds*. 2009;485(1-2):478-483. DOI: 10.1016/j.jallcom.2009.05.152

32. Roy P, Berger S, Schmuki P. TiO_2 Nanotubes: Synthesis and Applications. *Angewandte Chemie*. 2011;50(13):2904-2939. DOI: 10.1002/anie.201001374

33. Altomare M, Pozzi M, Allieta M, Bettini LG, Selli E. H_2 and O_2 photocatalytic production on TiO_2 nanotube arrays: Effect of the anodization time on structural features and photoactivity, *Applied Catalysis B: Environmental*. 2013;136-137:81-88. DOI: 10.1016/j.apcatb.2013.01.054

34. Wang C, Chen D, Ping G, Liu S, Huang X, Huang Y, et al. Controllable synthesis of well-ordered TiO_2 nanotubes in a mixed organic electrolyte for high-efficiency photocatalysis. *Science China Chemistry*. 2012;55(11):2373-2380. DOI: 10.1007/s11426-012-4680-0

35. Nischk M, Mazierski P, Gazda M, Zaleska A. Ordered TiO_2 nanotubes: The effect of preparation parameters on the photocatalytic activity in air purification process. *Applied Catalysis B: Environmental*. 2014;144:674-685. DOI: 10.1016/j.apcatb.2013.07.041

36. Roman I, Trusca RD, Soare ML, Fratila C, Krasicka-Cydzik E, Stan MS, et al. Titanium dioxide nanotube films: Preparation, characterization and electrochemical biosensitivity towards alkaline phosphatase. *Materials Science and Engineering: C*. 2014;37:374-382. DOI: 10.1016/j.msec.2014.01.036

37. Macak JM, Schmuki P. Anodic growth of self-organized anodic TiO_2 nanotubes in viscous electrolytes. *Electrochimica Acta*. 2006;52(3):1258-1264. DOI: 10.1016/j.electacta.2006.07.021

38. Albu SP, Ghicov A, Aldabergenova S, Drechsel P, LeClere D, Thompson GE, et al. Formation of Double-Walled TiO_2 Nanotubes and Robust Anatase Membranes. *Advanced Materials*. 2008;20(21):4135-4139. DOI: 10.1002/adma.200801189

39. Macak JM, Tsuchiya H, Ghicov A, Yasuda K, Hahn R, Bauer S, et al. TiO_2 nanotubes: Self-organized electrochemical formation, properties and applications. *Current Opinion in Solid State and Materials Science*. 2007;11(1-2):3-18. DOI: 10.1016/j.cossms.2007.08.004

40. ASTM International. *ASTM F67-13 - Standard Specification for Unalloyed Titanium, for Surgical Implant Applications (UNS R50250, UNS R50400, UNS R50550, UNS R50700)*. West Conshohocken: ASTM International; 2013.

41. Kubelka P. New Contributions to the Optics of Intensely Light-Scattering Materials. Part II: Nonhomogeneous Layers. *Journal of the Optical Society of America*. 1954;44(4):330-335 DOI: 10.1364/JOSA.44.000330

42. Murphy AB. Band-gap determination from diffuse reflectance measurements of semiconductor films, and application to photoelectrochemical water-splitting. *Solar Energy Materials and Solar Cells*. 2007;91(14):1326-1337. DOI: 10.1016/j.solmat.2007.05.005

43. Chen Z, Dinh H, Miller E, eds. *Photoelectrochemical Water Splitting Standards, Experimental Methods, and Protocols*. New York: Springer; 2013.

44. Khan S, Santos MJL, Malfatti CF, Dupont J, Teixeira SR. Pristine Ta_3N_5 Nanotubes: Trap-Driven High External Biasing Perspective in Semiconductor/Electrolyte Interfaces. *Chemistry A European Journal*. 2016;22(51):18501-18511. DOI: 10.1002/chem.201603246

45. Khan S, Zapata MJM, Baptista DL, Gonçalves RV, Fernandes JA, J. Dupont J, et al. Effect of Oxygen Content on the Photoelectrochemical Activity of Crystallographically Preferred Oriented Porous Ta_3N_5 Nanotubes. *The Journal of Physical Chemistry C*. 2015;119(34):19906-19914. DOI: 10.1021/acs.jpcc.5b05475

46. Smith YR, Ray RS, Carlson K, Sarma B, Misra M. Self-Ordered Titanium Dioxide Nanotube Arrays: Anodic Synthesis and Their Photo/Electro-Catalytic Applications. *Materials*. 2013;6(7):2892-2957. DOI: 10.3390/ma6072892

47. Munirathinam B, Pydimukkala H, Ramaswamy N. Neelakantan L. Influence of crystallite size and surface morphology on electrochemical properties of annealed TiO_2 nanotubes. *Applied Surface Science*. 2015;355:1245-1253. DOI: 10.1016/j.apsusc.2015.08.017

48. Grimes CA, Mor KK. *TiO_2 Nanotube Arrays*. New York: Springer; 2009.

49. Macak JM, Hildebrand H, Marten-Jahns U, Schmuki P. Mechanistic aspects and growth of large diameter self-organized TiO_2 nanotubes. *Journal of Electroanalytical Chemistry*. 2008;621(2):254-266. DOI: 10.1016/j.jelechem.2008.01.005

50. Kim D, Ghicov A, Schmuki P. TiO_2 Nanotube arrays: Elimination of disordered top layers ("nanograss") for improved photoconversion efficiency in dye-sensitized solar cells. *Electrochemistry Communications*. 2008;10(12):1835-1838. DOI: 10.1016/j.elecom.2008.09.029

51. Song YY, Lynch R, Kim D, Roy P, Schmuki P. TiO_2 Nanotubes: Efficient Suppression of Top Etching during Anodic Growth: Key to Improved High Aspect Ratio Geometries Corrosion, Passivation, and Anodic Films. *Electrochemical and Solid-State Letters*. 2009;12(7):C17-C20.

52. Albu SP, Schmuki P. Highly defined and ordered top-openings in TiO_2 nanotube arrays. *Physica Status Solidi - Rapid Research Letters*. 2010;4(7):151-153. DOI: 10.1002/pssr.201004159

53. Liao Y, Zhang D, Wang Q, Wen T, Jia L, Zhong Z, et al. Open-top TiO_2 nanotube arrays with enhanced photovoltaic and photochemical performances *via* a micromechanical cleavage approach. *Journal of Materials Chemistry A*. 2015;3(27):14279-14283. DOI: 10.1039/c5ta02799c

54. Vaenas N, Stergiopoulos T, Kontos AG, Likodimos V, Boukos N, Falaras P. Sensitizer activated solar cells based on self-organized TiO_2 nanotubes. *Microelectronic Engineering*. 2012;90:62-65. DOI: 10.1016/j.mee.2011.03.002

55. So S, Hwang I, Schmuki P. Hierarchical DSSC structures based on "single walled" TiO2 nanotube arrays reach a back-side illumination solar light conversion efficiency of 8%. *Energy & Environmental Science*. 2015;8(3):849-854. DOI: 10.1039/C4EE03729D

56. Yasuda K, Macak JM, Berger S, Ghicov A, Schmuki P. Mechanistic Aspects of the Self-Organization Process for Oxide Nanotube Formation on Valve Metals. *Journal of The Electrochemical Society*. 2007;154(9):C472-C478. DOI: 10.1149/1.2749091

57. Habazaki H, Fushimi K, Shimizu K, Skeldon P, Thompson GE. Fast migration of fluoride ions in growing anodic titanium oxide. *Electrochemistry Communications*. 2007;9(5):1222-1227. DOI: 10.1016/j.elecom.2006.12.023

58. Beranek R, Tsuchiya H, Sugishima T, Macak JM, Taveira L, Fujimoto S, et al. Enhancement and limits of the photoelectrochemical response from anodic TiO_2 nanotubes. *Applied Physics Letters*. 2005;87(24):243114. DOI: 10.1063/1.2140085

59. Zhang Z, Wang P. Optimization of photoelectrochemical water splitting performance on hierarchical TiO2 nanotube arrays. *Energy & Environmental Science*. 2012;5(4):6506-6512. DOI: 10.1039/c2ee03461a

60. Choudhury B, Bayan S, Choudhury A, Chakraborty P. Narrowing of band gap and effective charge carrier separation in oxygen deficient TiO_2 nanotubes with improved visible light photocatalytic activity. *Journal of Colloid and Interface Science*. 2016;465:1-10. DOI: 10.1016/j.jcis.2015.11.050

61. Fu Y, Du H, Zhang S, Huang W. XPS characterization of surface and interfacial structure of sputtered TiNi films on Si substrate. *Materials Science and Engineering: A*. 2005;403(1-2):25-31. DOI: 10.1016/j.msea.2005.04.036

62. Barsoukov E, Macdonald JR, eds. *Impedance Spectroscopy: Theory, Experiment and Applications*. 2nd Ed. Hoboken: John Wiley & Sons; 2005.

63. Lvovich VF. *Impedance Spectroscopy - Applications to Electrochemical and Dielectric Phenomena*. Hoboken: John Wiley & Sons; 2012. 368 p.

64. Gabrielli C. *Identification of Electrochemical Processes by Frequency Response Analysis.* Paris: Solartron Analytical; 1998.